TWO-MODE NONLINEAR STABILITY ANALYSIS

Hyun-Gull Yoon

Agency for Defense Development
4-4-1, Yuseong P.O.Box 35-4, Taejeon, Korea

ABSTRACT

A nonlinear mathematical model of longitudinal combustion instability appropriate for ramjets and augmentors was developed based on modal analysis. The model was limited to a two-mode formulation. The associated differential equations were solved both analytically and numerically and used to perform parametric studies.

1. Introduction

In the development of ramjet and afterburner combustion systems, one of the major concerns is the creation of large amplitude pressure oscillations by unsteady combustion. These self-excited oscillations (referred to as combustion instabilities) are driven by a coupling between the unsteady heat release and an acoustic oscillation at one of the resonant modes of the system.

Low frequency oscillations in the range of 50-500 Hz and generally characterized by longitudinal modes at the resonant frequencies of the combustor seem to be the most important in ramjet and afterburner combustion chambers. Several investigators such as Culick (1988), Langhorne (1988), Bloxsidge, Dowling, and Langhorne (1988), and Shyy and Udaykumar (1990) have suggested that these instabilities are primarily velocity sensitive.

For sufficiently strong excitations combustor oscillations become nonlinear. A mathematical model of nonlinear velocity-sensitive combustion instability is, therefore, necessary to predict ramjet and afterburner instabilities under such circumstances.

In this paper limited analytical work using a two-mode nonlinear model is conducted. Both approximate analytical solutions and direct numerical solutions are obtained. The modal amplitude equations are solved numerically under a variety of circumstances and a selection of numerical results is presented graphically.

2. Governing Equations

Consider a combustion chamber in the form of a duct of length L having an inlet at the left end. The combustion chamber contains a flowing mixture of fuel, oxidizer, and products of combustion which will be treated herein as an inviscid nonconducting ideal gas with gas constant R and ratio of specific heats γ. Treating the flow as one-dimensional, the respective conservation equations for mass, linear momentum, and total energy are

$$\frac{\partial \rho}{\partial t} + \rho\frac{\partial u}{\partial x} + u\frac{\partial \rho}{\partial x} = 0$$

$$\rho(\frac{\partial u}{\partial t} + u\frac{\partial u}{\partial x}) = -\frac{\partial p}{\partial x} + D \qquad (1)$$

$$\frac{\partial}{\partial t}[\rho(e + \frac{u^2}{2})] + \frac{\partial}{\partial x}[u\rho(e + \frac{u^2}{2}) + up] = Q$$

where x is axial position, t is time, ρ is density, u is axial velocity, p is pressure, D is axial body force per unit volume, e is specific internal energy, and Q is the heat addition rate per unit volume. The equations of state are

$$p = \rho RT, \qquad e = \frac{RT}{\gamma - 1} \qquad (2)$$

It is convenient to introduce dimensionless quantities by the following transformations

$$x \to Lx, \qquad t \to \frac{L}{c_i}t, \qquad \rho \to \rho_i(1+\bar{\rho}+\rho), \qquad u \to c_i(u_0+\bar{\phi}'+\frac{\partial \phi}{\partial x}),$$

$$p \to \frac{\rho_i c_i^2}{\gamma}(1+\bar{p}+p), \quad T \to \frac{c_i^2}{\gamma R}(1+\bar{T}+T), \quad D \to \frac{\rho_i c_i^2}{L}(\bar{A}'+\frac{\partial A}{\partial x}), \quad Q \to \frac{\rho_i c_i^3}{L}(\bar{Q}+Q) \qquad (3)$$

where the symbol $\to$ indicates a transition from dimensional quantities (tail) to corresponding dimensionless quantities (tip), a bar indicates a steady state quantity (function of x only), a prime indicates differentiation of a function of one variable with respect to its argument, ρ_i is the initial density, c_i is the initial sound speed, u_0 is the dimensionless inlet velocity, ϕ denotes velocity potential, and A denotes force potential. The dimensionless dependent variables are treated as small perturbations from a reference state characterized by unit pressure, temperature, density, and constant velocity u_0. Terms that are linear in the perturbations will be called first order terms, those quadratic in the perturbations second order terms, etc. It is desired to obtain a system of equations structured such that the first order terms will be those associated with the equations of linear acoustics and all additional effects (body force, heat addition, mean flow, nonlinearity) will appear as second order corrections. (This approach is similar to that of Culick (1988) and is motivated by observations that the disturbances associated with combustion instabilities usually closely resemble the acoustic modes of the chamber.) Toward this end u_0 will be treated as a first order term while the sources will be treated as second order terms. Substituting (3) into (1) and (2), retaining only first and second order terms, and carrying out a number of manipulations (omitted for the sake of brevity) yields

$$\frac{\partial^2 \phi}{\partial t^2} - \frac{\partial^2 \phi}{\partial x^2} + 2u_0\frac{\partial^2 \phi}{\partial x \partial t} + 2\frac{\partial \phi}{\partial x}\frac{\partial^2 \phi}{\partial x \partial t} + (\gamma - 1)\frac{\partial \phi}{\partial t}\frac{\partial^2 \phi}{\partial x^2} - \frac{\partial A}{\partial t} + (\gamma - 1)Q = 0 \qquad (4)$$

for the stability problem. In (4) ξ and η are dummy variables. Since $\bar{Q}$ is a second order term according to the original assumptions, $\bar{u}$ is predicted to be a second order term (rather than first order as originally assumed) while $\bar{\rho}$ and $\bar{T}$ are predicted to be first order terms.

In the present work the heat addition term Q will be used to account for the burning process and the body force term A will be used to approximately represent the ability of devices such as baffles and liners to modify the frequency and damping characteristics of the system. These latter effects cannot be handled exactly in a one-dimensional formulation.

3. Nonlinear Stability Analysis

Assuming

$$A = -\eta\phi - k\int\phi\,dt \tag{5}$$

(η and k being constants)
the wave equation (4) which includes nonlinear terms is

$$\frac{\partial^2\phi}{\partial t^2} - \frac{\partial^2\phi}{\partial x^2} + 2u_0\frac{\partial^2\phi}{\partial x\partial t} + 2\frac{\partial\phi}{\partial x}\frac{\partial^2\phi}{\partial x\partial t} + (\gamma-1)\frac{\partial\phi}{\partial t}\frac{\partial^2\phi}{\partial x^2} + \eta\frac{\partial\phi}{\partial t} + k\phi + (\gamma-1)Q = 0\,. \tag{6}$$

In (5) the terms multiplied by k and η play the roles of respective generic frequency change and damping effects not associated with either combustion or mean flow. To illustrate some of the effects of nonlinearity in a relatively simple way, a two-mode solution will be discussed herein.

A two-mode model can be developed by assuming an approximate solution of (6) in the form

$$\phi = \epsilon\,[\,f_1(t)\,\psi_1(x) + f_2(t)\,\psi_2(x)\,] \tag{7}$$

where ϵ is a dimensionless measure of the initial disturbance amplitude. For the nonlinear analysis the idealized burning-rate expression

$$Q = \overline{Q}\,\{\,Y_1 u(x,t-\tau) + Y_2 u^2(x,t-\tau)\,\} \tag{8}$$

will be used which incorporates both the linear and the nonlinear velocity-sensitive terms. For simplicity, the amplification factors Y_1 and Y_2 are assumed to be constant.

Substituting (7) and (8) into (6), and using the modal analysis procedure leads to

$$\begin{aligned}&\ddot{f}_1 + (\eta + 2u_0C_{11})\dot{f}_1 + 2u_0C_{21}\dot{f}_2 + (\Omega_1^2 + k)f_1\\ &+ \epsilon\,(\,C_{111}f_1\dot{f}_1 + C_{121}f_1\dot{f}_2 + C_{211}\dot{f}_1f_2 + C_{221}f_2\dot{f}_2\,)\\ &+ (\gamma-1)\{\,Y_1[\,D_{11}f_1(t-\tau) + D_{21}f_2(t-\tau)\,]\\ &+ \epsilon Y_2[\,D_{111}f_1^2(t-\tau) + 2D_{121}f_1(t-\tau)f_2(t-\tau) + D_{221}f_2^2(t-\tau)\,]\,\} = 0\end{aligned} \tag{9}$$

and

$$\begin{aligned}&\ddot{f}_2 + (\eta + 2u_0C_{22})\dot{f}_2 + 2u_0C_{12}\dot{f}_1 + (\Omega_2^2 + k)f_2\\ &+ \epsilon\,(\,C_{112}f_1\dot{f}_1 + C_{122}f_1\dot{f}_2 + C_{212}\dot{f}_1f_2 + C_{222}f_2\dot{f}_2\,)\\ &+ (\gamma-1)\{\,Y_1[\,D_{12}f_1(t-\tau) + D_{22}f_2(t-\tau)\,]\\ &+ \epsilon Y_2[\,D_{112}f_1^2(t-\tau) + 2D_{122}f_1(t-\tau)f_2(t-\tau) + D_{222}f_2^2(t-\tau)\,]\,\} = 0\end{aligned} \tag{10}$$

where

$$C_{ijk} = \int_0^1[\,2\psi_i'\psi_j' - (\gamma-1)\Omega_i^2\psi_i\psi_j\,]\,\psi_k\,dx\,, \qquad D_{ijk} = \int_0^1\overline{Q}\;\psi_i'\psi_j'\psi_k\,dx\,. \tag{11}$$

Equations (9) and (10) are a pair of coupled second-order nonlinear differential equations governing the modal amplitudes f_1 and f_2. It can be seen that both the nonlinear gas dynamics terms (multiplied by the C's) and the nonlinear combustion response terms (multiplied by the D's) produce modal coupling.

Before discussing the numerical solution of these equations, it is of interest to illustrate a fundamental behavior introduced by the nonlinear velocity-sensitive combustion response. Toward this end the nonlinear gas dynamics terms will be ignored ($C_{ijk} = 0$), mean flow effects will be neglected ($u_0 = 0$), the combustion response will be assumed to be purely quadratic with zero time delay ($Y_1 = 0$, $\tau = 0$), and the combustion will be assumed to be uniformly distributed ($\overline{Q} = 1$). For closed/closed conditions ($\psi_n = \sqrt{2}\cos(n\pi x)$, $\Omega_n = n\pi$; $n = 1, 2$) (9) and (10) become

$$\ddot{f}_1 + \eta\dot{f}_1 + \pi^2 f_1 + 2\sqrt{2}\pi^2(\gamma-1)\epsilon Y_2 f_1 f_2 = 0$$
$$\ddot{f}_2 + \eta\dot{f}_2 + 4\pi^2 f_2 - \sqrt{2}\pi^2(\gamma-1)\epsilon Y_2 f_1^2 = 0 . \tag{12}$$

An approximate closed form solution to these equations will be found as follows. Assume

$$f_n = A_n(t)\cos(n\pi t) + B_n(t)\sin(n\pi t) \quad ; \quad n = 1,2 . \tag{13}$$

Substituting (13) and its time derivatives into (12) and ordering the terms yields

$$[2\pi\dot{B}_1 + \pi\eta B_1 + \sqrt{2}\pi^2\epsilon(\gamma-1)Y_2(A_1A_2 + B_1B_2)]\cos(\pi t)$$
$$+ [-2\pi\dot{A}_1 - \pi\eta A_1 + \sqrt{2}\pi^2\epsilon(\gamma-1)Y_2(A_1B_2 - A_2B_1)]\sin(\pi t) + \cdots = 0$$
$$[4\pi\dot{B}_2 + 2\pi\eta B_2 - \frac{\sqrt{2}}{4}\pi^2\epsilon(\gamma-1)Y_2(A_1^2 - B_1^2)]\cos(2\pi t) \tag{14}$$
$$+ [-4\pi\dot{A}_2 - 2\pi\eta A_2 - \frac{\sqrt{2}}{2}\pi^2\epsilon(\gamma-1)Y_2A_1B_1]\sin(2\pi t) + \cdots = 0$$

where $+\cdots$ indicates all terms involving harmonics other than the dominant one. Neglecting these terms requires that

$$\dot{A}_1 + \frac{\eta}{2}A_1 - \frac{\sqrt{2}}{2}\pi\varepsilon(\gamma-1)Y_2(A_1B_2 - A_2B_1) = 0$$
$$\dot{B}_1 + \frac{\eta}{2}B_1 + \frac{\sqrt{2}}{2}\pi\varepsilon(\gamma-1)Y_2(A_1A_2 + B_1B_2) = 0$$
$$\dot{A}_2 + \frac{\eta}{2}A_2 + \frac{\sqrt{2}}{8}\pi\varepsilon(\gamma-1)Y_2A_1B_1 = 0 \tag{15}$$
$$\dot{B}_2 + \frac{\eta}{2}B_2 - \frac{\sqrt{2}}{16}\pi\varepsilon(\gamma-1)Y_2(A_1^2 - B_1^2) = 0 .$$

These are four coupled differential equations to be solved for the slowly varying amplitudes A_1, A_2, B_1, and B_2. Similar equations would be obtained by using the more formal method of multiple scales (see Nayfeh [4]). These equations cannot be solved in closed form for all situations. One special case in which a closed form solution is possible will be discussed herein.

It can be observed that

$$A_1 = A_2 = 0 \tag{16}$$

satisfies (15), and reduces these equations to

$$\begin{aligned} \dot{B}_1 + \frac{\eta}{2}B_1 + \frac{\sqrt{2}}{2}\pi\epsilon(\gamma-1)Y_2B_1B_2 &= 0 \\ \dot{B}_2 + \frac{\eta}{2}B_2 + \frac{\sqrt{2}}{16}\pi\epsilon(\gamma-1)Y_2B_1^2 &= 0. \end{aligned} \tag{17}$$

It can be shown (with the details being omitted for the sake of brevity) that these equations have the closed form solutions

$$\begin{aligned} B_1 &= e^{-\frac{\eta}{2}t}\sec\left[\frac{\pi}{2\eta}\epsilon(\gamma-1)Y_2(1 - e^{-\frac{\eta}{2}t})\right] \\ B_2 &= -\frac{\sqrt{2}}{4}e^{-\frac{\eta}{2}t}\tan\left[\frac{\pi}{2\eta}\epsilon(\gamma-1)Y_2(1 - e^{-\frac{\eta}{2}t})\right]. \end{aligned} \tag{18}$$

It is observed that (18) satisfy the initial conditions

$$B_1(0) = 1\,, \quad B_2(0) = 0\,. \tag{19}$$

Thus, from (13), $f_1(0) = 0$, $\dot{f}_1(0) = \pi$, $f_2(0) = 0$, and $\dot{f}_2(0) = 0$. Substituting (18) into (13) yields

$$\begin{aligned} f_1 &= e^{-\frac{\eta}{2}t}\sec\left[\frac{\pi}{2\eta}\epsilon(\gamma-1)Y_2(1 - e^{-\frac{\eta}{2}t})\right]\sin(\pi t) \\ f_2 &= -\frac{\sqrt{2}}{4}e^{-\frac{\eta}{2}t}\tan\left[\frac{\pi}{2\eta}\epsilon(\gamma-1)Y_2(1 - e^{-\frac{\eta}{2}t})\right]\sin(2\pi t). \end{aligned} \tag{20}$$

Substituting (20) into (7) yields the final result

$$\begin{aligned} \phi = {} & \sqrt{2}\,e^{-\frac{\eta}{2}t}\sec\left[\frac{\pi}{2\eta}\epsilon(\gamma-1)Y_2(1 - e^{-\frac{\eta}{2}t})\right]\epsilon\sin(\pi t)\cos(\pi x) \\ & - \frac{1}{2}e^{-\frac{\eta}{2}t}\tan\left[\frac{\pi}{2\eta}\epsilon(\gamma-1)Y_2(1 - e^{-\frac{\eta}{2}t})\right]\epsilon\sin(2\pi t)\cos(2\pi x). \end{aligned} \tag{21}$$

Inspection of (18) shows that both B_1 and B_2 will eventually decay to zero for $Y_2 < \eta / [\epsilon(\gamma - 1)]$ but will reach infinity in a finite time for $Y_2 > \eta / [\epsilon(\gamma - 1)]$. Thus the value of Y_2 corresponding to neutral stability is

$$Y_2 = \frac{\eta}{\epsilon(\gamma - 1)}. \tag{22}$$

Typical results for B_1 and B_2 are shown in Figure 1 (stable case) and Figure 2 (unstable case). For the parametric values associated with these figures, (22) yields $Y_2 = 5.0$. It is interesting to note from Figure 2 that the first mode initially decays and then grows. Energy from the first mode is first transferred to the second mode, causing it to grow. Then energy is transferred back to the first mode, causing it to grow also. This "bootstrapping" effect is the basic mechanism of nonlinear velocity-sensitive combustion instability. This mechanism is clearly contained within the present model.

The fact that the first mode exhibits initial decay even for ultimately unstable cases has an interesting implication for linear stability models. Such models investigate only the initial behavior of small disturbances. Thus a linear stability analysis would always indicate stability in the case of bootstrapping and completely miss the ultimate behavior. This is one reason why a nonlinear model is needed to investigate velocity-sensitive combustion response. It appears to be the rectification effect produced by the second term on the right-hand side of (8) which is fundamental to bootstrapping. A similar rectification effect will be produced by any combustion response exhibiting a Reynolds number dependence (typical of convection processes). The quadratic form employed in (8) was chosen because it is the analytically simplest form which allows for rectification. The relative values of Y_1 and Y_2 can be adjusted to approximate the response of other Reynolds number dependant responses.

To obtain complete solutions to (12) requires numerical computation. In the present work a standard fourth order Runge-Kutta procedure was employed with the modification that time delayed terms were treated as known functions of time. Because of time delay, initial conditions must be stated in the interval $-\tau < t < 0$. Quiescent conditions were always assumed in the present work.

4. Parametric Studies

This section reports on several parametric studies. In all cases closed/closed acoustic boundary conditions are assumed and the parametric values $u_0 = 0$, $k = 0$, $\gamma = 1.2$, $\eta = 0.1$ are employed. Equations (9) and (10) are solved numerically to produce the predictions. In these equations the terms multiplied by C's represent nonlinear gas dynamics effects and those multiplied by D's are associated with the combustion response. It is of interest to determine the importance of the nonlinear gas dynamics effects. Toward this end some simulations were carried out using (9) and (10) with all C's equated to zero. These will be labeled D. Other simulations were performed using the complete form of (9) and (10). These will be labeled CD. All of the calculations were performed with a time step $\Delta t = 0.01$. The initial conditions employed were

$$f_1(0) = 1 \ , \ \dot{f}_1(0) = 0 \ , \ f_2(0) = 0 \ , \ \dot{f}_2(0) = 0 \ . \tag{23}$$

Table 1 shows the stability predictions for four related D and CD cases involving uniform combustion. It can be seen that the inclusion of the nonlinear gas dynamics effects in the model can have an important influence. This becomes more apparent from inspection of Figures 3-6. Figures 3 (D) and 4 (CD) both show stable behavior but exhibit considerable disagreement as to the behavior of the modal amplitudes. Figures 5 (D) and 6 (CD) show even more disagreement in that the former exhibits unstable behavior while the latter exhibits marginally stable behavior. It is possible, of course, that extending the calculation illustrated in Figure 6 for a sufficiently long time period would ultimately reveal unstable behavior. This demonstrates one of the difficulties of nonlinear stability analysis. The stability predictions may depend on the time interval chosen for the simulations.

Table 2 presents stability predictions for purely quadratic combustion response with no time delay based on the CD model. The influences on the predictions of the source location and the combustion strength are illustrated. The pattern of predictions appears to be symmetric about the centerline. For a given location the system becomes more unstable as the combustion strength is increased. No location appears to be completely free of instability. Figures 7 and 8 show representative stable (Figure 7) and unstable (Figure 8) behaviors with the source at the chamber center. These predictions illustrate the ability of the model to quickly estimate the effect of changes in the source position.

Table 3 contains predictions corresponding to Table 2 made using the D model. The same pattern of symmetry about the centerline is exhibited. There are, however, a number of differences in the stability predictions. This illustrates the importance of retaining the nonlinear gas dynamics effects.

5. Conclusion

In this paper a nonlinear mathematical model of longitudinal combustion instability appropriate for ramjets and augmentors was developed based on modal analysis. The model was limited to a two-mode formulation. The two-mode nonlinear model is capable of predicting the bootstrapping effect which characterizes nonlinear velocity-sensitive combustion response. It is, therefore, a useful vehicle for parametric studies designed to determine the influence of combustion distribution on stability behavior. It can be extended in a straightforward way to an arbitrary number of modes at the cost of escalating computational effort.

The combustion response function (8) is an idealization chosen for analytical convenience. Real nonlinear velocity-sensitive response is described by more complex functions which do not lend themselves to modal analysis. An alternative to the modeling is to employ an analog experimental system in which a hotwire anemometer plays the role of the velocity-sensitive element.

References

[1] Bloxsidge, G.J., Dowling, A.P., and Langhorne, P.J., 1988, "Reheat buzz: an acoustically coupled combustion instability. Part 2. Theory," *Journal of Fluid Mechanics*, Vol. 193, pp. 445-473.

[2] Culick, F.E.C., 1988, "Combustion Instabilities in Liquid-Fueled Propulsion Systems - An Overview," *AGARD Conference Proceedings* - 450.

[3] Langhorne, P.J., 1988, "Reheat buzz: an acoustically coupled combustion instability. Part 1. Experiment," *Journal of Fluid Mechanics*, Vol. 193, pp. 417-443.

[4] Nayfeh, A.H., 1973, *Perturbation Methods*, A Wiley-Interscience Publication, 1973.

[5] Shyy, W. and Udaykumar, H., 1990, "Numerical Simulation of Thermo-Acoustic Effect on Longitudinal Combustion Instabilities," *A Paper AIAA 90-2065, Presented at the 26th Joint Propulsion Conference*, Orlando, Florida.

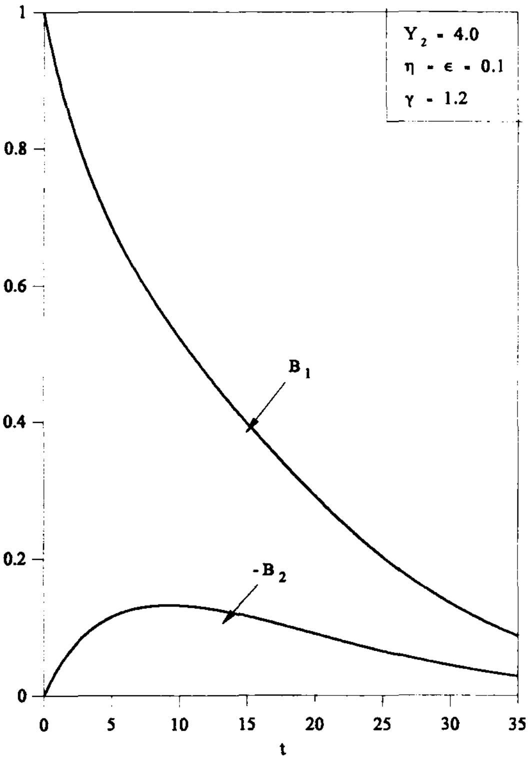

Figure 1. Amplitude histories predicted by perturbation solution (stable case)

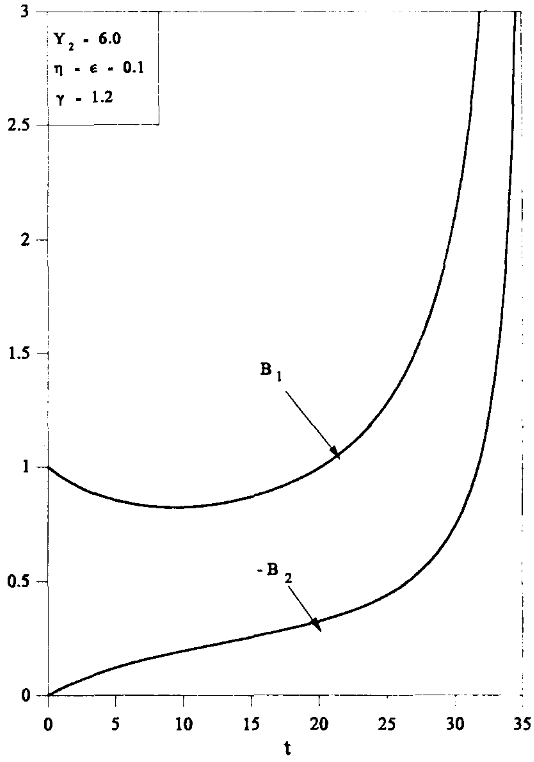

Figure 2. Amplitude histories predicted by perturbation solution (unstable case)

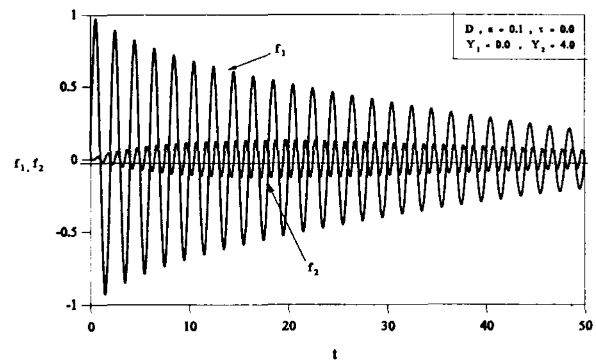

Figure 3. Runge-Kutta modal amplitude predictions for uniform combustion ($\overline{Q}$ = 1, D, Y_2 = 4.0)

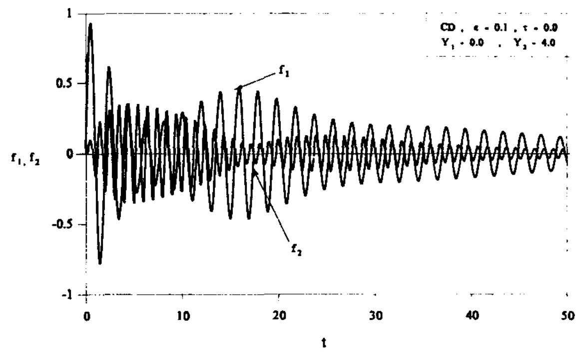

Figure 4. Runge-Kutta modal amplitude predictions for uniform combustion ($\overline{Q}$ = 1, CD, Y_2 = 4.0)

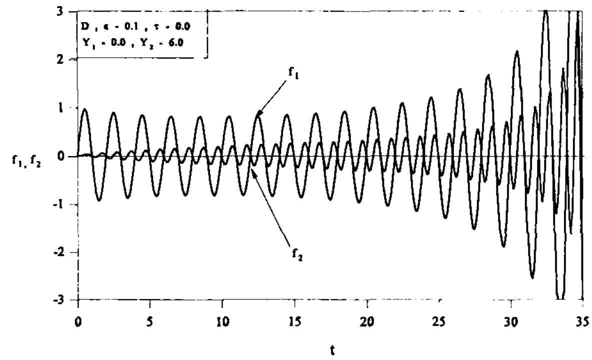

Figure 5. Runge-Kutta modal amplitude predictions for uniform combustion ($\bar{Q}$ = 1, D, Y_2 = 6.0)

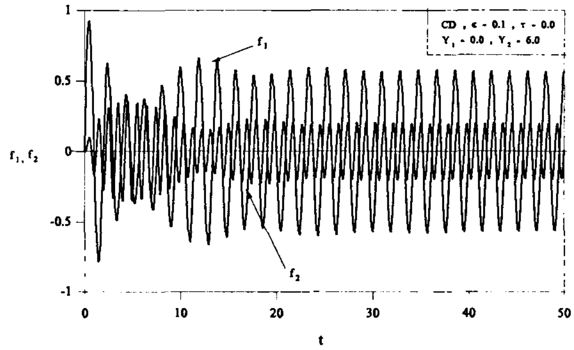

Figure 6. Runge-Kutta modal amplitude predictions for uniform combustion ($\bar{Q}$ = 1, CD, Y_2 = 6.0)

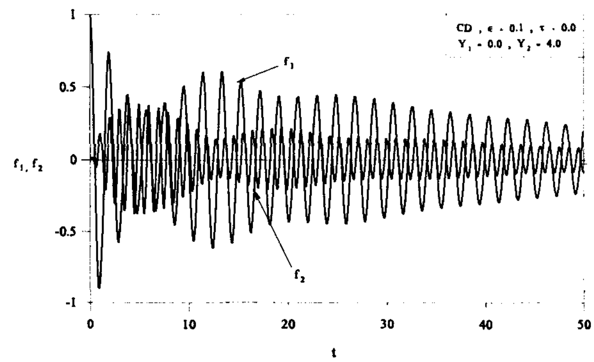

Figure 7. Runge-Kutta modal amplitude predictions for unit concentrated combustion ($\bar{Q}$ = Δ(x - 0.5), Y_1 = 0.0, Y_2 = 4.0)

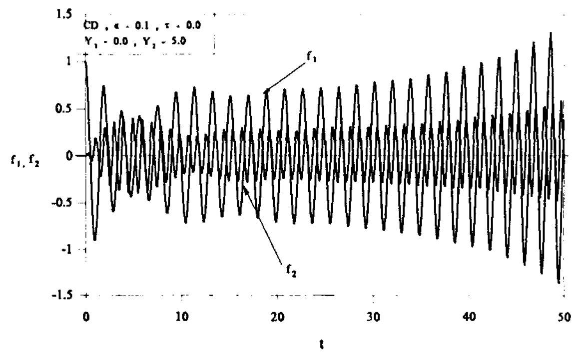

Figure 8. Runge-Kutta modal amplitude predictions for unit concentrated combustion ($\bar{Q}$ = Δ(x - 0.5), Y_2 = 5.0)

Table 1. Stability predictions for uniform combustion ($\bar{Q}$ = 1, ϵ = 0.1 , τ = 0.0, Y_1 = 0.0)

Y_2	4.0	5.0	6.0	7.0
D	+	+	-	-
CD	+	+	+	-

Table 2. Stability predictions for unit concentrated combustion ($\overline{Q} = \Delta(x - \lambda)$, CD, $\epsilon = 0.1$ $Y_1 = 0.0$, $\tau = 0.0$)

Y_2 \ λ	0.2	0.4	0.5	0.6	0.8
2.0	+	+	+	+	+
4.0	+	+	+	+	+
4.5	+	-	+	-	+
5.0	+	-	-	-	+
5.5	+	-	-	-	+
6.0	+	-	-	-	+
8.0	-	-	-	-	-

Table 3. Stability predictions for unit concentrated combustion ($\overline{Q} = \Delta(x - \lambda)$, D, $\epsilon = 0.1$, $Y_1 = 0.0$, $\tau = 0.0$)

Y_2 \ λ	0.2	0.4	0.5	0.6	0.8
2.0	+	+	+	+	+
4.0	+	-	+	-	+
4.5	+	-	+	-	+
5.0	+	-	+	-	+
5.5	+	-	+	-	+
6.0	+	-	+	-	+
8.0	+	-	+	-	+